Jet physics and initial-state QCD parton showers[1]

F. Hautmann
Department of Theoretical Physics
University of Oxford, Oxford OX1 3NP

Abstract. We discuss methods of parton branching to treat corrections to QCD showers beyond the collinear ordering approximation in hadronic collisions at high energies. We illustrate the role of finite-angle gluon radiation for angular and momentum correlations in multi-jet final states, and describe applications to forward jets at the LHC.

1 Introduction

Complex final states containing multiple hadronic jets are produced copiously at the Large Hadron Collider (LHC), and enter in a number of new particle discovery processes that are central to the LHC physics program. In many of these processes the experimental capabilities to disentangle signal from background are significantly enhanced if the detailed structure of jets can itself be used as a diagnostics for potential new physics effects, e.g. in decays of highly boosted massive states. The interpretation of experimental data for such multi-particle final states relies both on perturbative multi-jet calculations and on realistic event simulation by parton-shower Monte Carlo generators.

Owing to the complex kinematics involving multiple hard scales and the large phase space opening up at LHC energies, multi-jet events are potentially sensitive to effects of QCD initial-state radiation that depend on the finite transverse-momentum tail of partonic matrix elements and distributions. These effects are not included in the branching algorithms of standard shower Monte Carlo event generators, based on collinear jet evolution. On the other hand, they are taken into account only partially in perturbative fixed-order calculations, order-by-order through higher-loop contributions. Such effects are present to all orders in α_s and can become logarithmically enhanced at high energy.

This article discusses methods to treat these effects and their role for the structure of jet final states, based on the works [1, 2]. We start in Sec. 2 with basic elements of the parton branching methods, focusing on corrections to collinear ordering in space-like parton showers at high energy. In Sec. 3 we give examples on jet-jet correlations and discuss the case of forward jet production at the LHC. We summarize in Sec. 4.

[1]Presented at *X Workshop on Nonperturbative QCD*, IAP, Paris, 2009.

2 Multi-parton emission by branching methods

A pp collision event at the LHC can be thought of as consisting of a hard scattering, parton showering, hadronization and a soft underlying process. The showering extends from short to long time scales, producing multiple parton emission. In this section we focus on this process and discuss branching methods to take into account different contributions to multi-parton radiation.

2.1 Collinear showering and soft gluon coherence

Branching algorithms in standard shower Monte Carlo generators [3] are based on collinear evolution of the jets, both time-like and space-like, developing from the hard event. The branching probability is given in terms of splitting functions P and form factors Δ (Fig. 1) as

$$d\mathcal{P} = \int \frac{dq^2}{q^2} \int dz \; \alpha_S(q^2) \; P(z) \; \Delta(q^2, q_0^2) \quad . \tag{1}$$

The theoretical basis for the branching approach is the factorizability of universal splitting functions in QCD cross sections in the collinear limit [4, 5], which justifies the probabilistic picture.

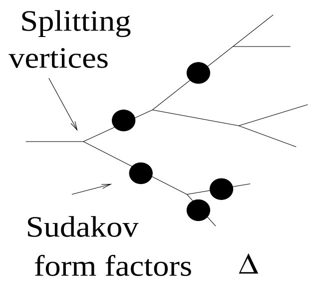

Figure 1: *Parton branching in terms of splitting probabilities and form factors.*

Besides small-angle, incoherent parton emission, shower generators (or more precisely some of them, see e.g. discussions in [6, 7]) also take into account further radiative contributions, associated with emission of soft gluons. These contributions are essential for realistic phenomenology [6, 7]. To incorporate them in a probabilistic framework, one appeals to properties of coherence of color charge radiation.

Recall [4, 8, 9] that soft-gluon emission amplitudes factorize in terms of eikonal currents [10, 11]

$$\mathbf{J}_\mu^a = \sum_{i=1}^{n} \mathbf{Q}_i^a \; \frac{p_{i\mu}}{p_i \cdot q} \quad , \tag{2}$$

where p_i are the emitters' momenta, q is the soft momentum, and the color charge operators $\mathbf{Q}_i^a$ are associated with the emission of gluon a from parton i. In general, interferences are expected to contribute to the radiative terms relating the $(n+1)$-parton process to the n-parton process. Nevertheless, a probabilistic branching-like picture can be recovered [12, 13, 14] by exploiting soft-gluon coherence.

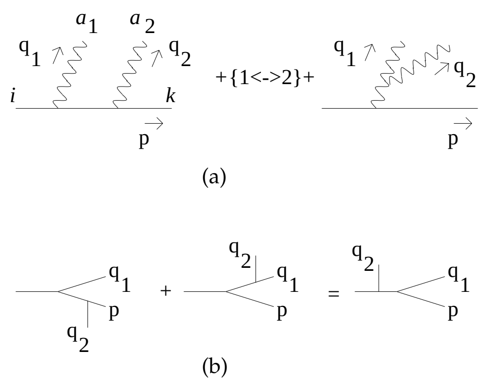

Figure 2: *(a) Two gluon emission from a fast quark; (b) coherence of soft gluon emission at large angle.*

In the single-emission case, gluon coherence can be characterized simply as a property of suitably defined azimuthal averages of the emission cross sections [13, 14]. At the multiple emission level, Fig. 2 illustrates the case of two soft gluons with momenta q_1 and q_2 produced from a fast parton with momentum p (Fig. 2a). Suppose $q_2^0 \ll q_1^0$. We distinguish two angular regions for the softest gluon q_2. i) When q_2 is at small angle from p (q_1), then the amplitude can be seen as the sequential emission of q_1 from p and of q_2 from p (q_1). This corresponds to the standard bremsstrahlung picture based on radiation cones centered around p and q_1. ii) When q_2 is at large angle, $\theta_{pq_2} \gg \theta_{pq_1}$, then the directions of p and q_1 can be identified and the two emission amplitudes act coherently to give (Fig. 2b) what can be seen as the sequential emission of q_2 from p and of q_1 from p. The reversed order of the emissions compared to case i) reflects the fact that the radiated gluon sees the total color charge of the emitting jet.

Fig. 2b illustrates that the contributions of different emitters combine so as to give an effective contribution in which the emissions are ordered in angle. Angular ordering [12, 13, 14] thus replaces energy ordering: in the right hand side of Fig. 2b the gluon emitted first is no longer the hardest.

2.2 Space-like parton shower at high energies

The arguments used in the previous subsection take into account, through the current (2), soft vector emission from external lines in parton scattering amplitudes, and are fully appropriate for scattering problems characterized by a single hard scale [4]. New effects come about, however, when one tries to extend this picture to processes at increasingly high energies with multiple hard scales, such as at the LHC. On one hand, emissions in the parton branching that are not collinearly ordered become non-negligible; on the other hand, coherence sets in from emissions due to internal space-like lines in the branching decay chain [15, 16, 17].

More precisely, the first observation to address the high energy kinematics is that soft-gluon insertion rules [8, 13] for n-parton scattering amplitudes $M^{(n)}$ can still be given in terms of real and virtual soft-gluon currents $\mathbf{J}^{(R)}$ and $\mathbf{J}^{(V)}$,

$$
\begin{aligned}
\left|M^{(n+1)}(k,p)\right|^2 \; &= \; \Big\{ [M^{(n)}(k+q,p)]^\dagger \; [\mathbf{J}^{(R)}]^2 \; M^{(n)}(k+q,p) \\
&- \; [M^{(n)}(k,p)]^\dagger \; [\mathbf{J}^{(V)}]^2 \; M^{(n)}(k,p) \Big\} \quad , \qquad (3)
\end{aligned}
$$

but the currents are modified in the high-energy, multi-scale region by terms that depend on the total transverse momentum transmitted down the initial-state parton decay chain [15, 16, 17]. As a result, the physically relevant distribution to describe initial-state showers becomes the analogue not so much of an ordinary parton density but rather of an "unintegrated" parton density, dependent on both longitudinal and transverse momenta.[2]

The next observation concerns the structure of virtual corrections. Besides Sudakov form-factor effects included in standard shower algorithms [3, 4], one needs in general virtual-graph terms to be incorporated in transverse-momentum dependent (but universal) splitting functions [15, 23, 24, 25] in order to take account of gluon coherence not only for collinear-ordered emissions but also in the non-ordered region that opens up at high $\sqrt{s}/p_\perp$, where $\sqrt{s}$ is the total center-of-mass energy and $p_\perp$ is the typical transverse momentum of a produced jet.

The resulting structure of the parton branching, depicted in Fig. 3, differs from that in Eq. (1). The kernels $\mathcal{P}$ depend on transverse momenta and include part of the virtual corrections, in such a way as to avoid double counting with the Sudakov form factor Δ, while reconstructing color coherence not only at large x but also at small x [26] in the angular region (Fig. 3)

$$\alpha/x > \alpha_1 > \alpha \quad , \qquad (4)$$

where the angles α for the partons radiated from the initial-state shower are taken with respect to the initial beam jet direction, and increase with increasing off-shellness.

From the standpoint of higher-order corrections, the effects of region (4) are potentially enhanced by terms

$$\alpha_s^k \ln^{k+m} \sqrt{s}/p_\perp \quad . \qquad (5)$$

[2]See [18] for recent reviews of unintegrated pdfs. Aspects of u-pdfs from the standpoint of QCD high-energy factorization are discussed in [19]. Recent applications to phenomenology may be found in [20, 21, 22]. The papers in [23] contain first discussions of a more general, nonlocal operator formulation of u-pdfs applied to parton showers beyond leading order.

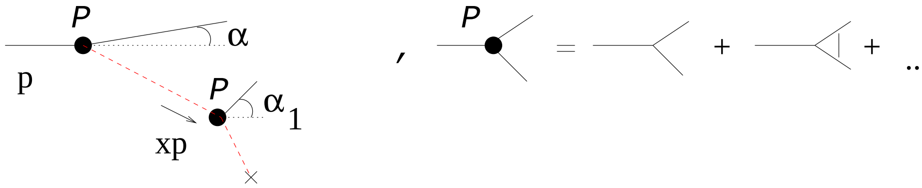

Figure 3: *(left) Coherent radiation in the space-like parton shower for $x \ll 1$; (right) the unintegrated splitting function $\mathcal{P}$, including small-x virtual corrections.*

In inclusive processes, coherence leads to strong cancellations between reals and virtuals so that terms with $m \geq 1$ in Eq. (5) drop out [27, 24]. As a result, for instance, the anomalous dimensions γ^{ij} for the evolution of the space-like jet receive at most single-logarithmic corrections at high energy [24, 28, 29]. For exclusive jet distributions such cancellations are not present and one may expect stronger enhancements. The implementation of coherent effects associated with high-energy logarithms is, from the point of view of jet physics, the main motivation for developing the formalism of unintegrated parton distributions and implementing it in shower Monte Carlo event generators.

The finite-$k_\perp$ corrections to high-energy space-like showers discussed above affect the structure of jet correlations and multiplicity distributions in multi-particle final states. We discuss examples in the next section.

3 Applications to jet final states

This section discusses applications of the transverse momentum dependent parton branching to jet physics. We start with results for angular and momentum correlations in multi-jet final states observed, at central rapidities, in $p\bar{p}$ and ep collisions. We then consider a new area of measurements that will open up at the LHC, involving events that are both high-$p_\perp$ and forward. Using forward detectors, experiments will be able to measure azimuthal plane correlations between jets across intervals of five units or more in rapidity. We discuss ongoing work in this area.

3.1 Angular correlations in multi-jet final states

In a multi-jet event the correlation in the azimuthal angle $\Delta\phi$ between the two hardest jets provides a useful measurement, sensitive to how well QCD multiple-radiation effects are described. In leading order one expects two back-to-back jets; higher-order radiative contributions cause the $\Delta\phi$ distribution to spread out. Near $\Delta\phi \sim \pi$ the measurement is mostly sensitive to infrared effects from soft-gluon emission; the behavior as $\Delta\phi$ decreases is driven by hard parton radiation. At the LHC such measurements can be used to test the description of complex hadronic final states by Monte Carlo generators.

Experimental data on $\Delta\phi$ correlations are available at present from the Tevatron [30] and from Hera [31, 32]. The comparison with shower Monte Carlo results and perturbative results are very different in the two cases. The Tevatron $\Delta\phi$ distribution drops by about two orders of magnitude over a fairly narrow range, essentially still close to the two-jet region. The measurement is dominated by leading-order processes, with small sub-leading corrections. Correspondingly, data are reasonably well described both by collinear showers (Herwig and the new tuning of Pythia) and by fixed-order NLO calculations [30, 33].

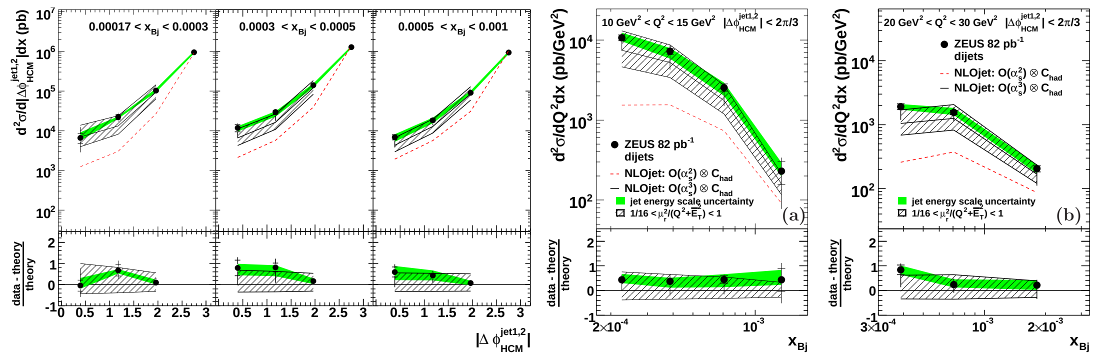

Figure 4: *(left) Azimuth dependence and (right) Bjorken-x dependence of ep di-jet distributions [31], compared with NLO results.*

The Hera $\Delta\phi$ measurements, on the other hand, are much more sensitive to higher order radiative effects, see Fig. 4 [31]. NLO results for di-jet azimuthal distributions are affected by large corrections in the small-$\Delta\phi$ and small-x region, and begin to fall below the data for three-jet distributions in the smallest $\Delta\phi$ bins [31]. These measurements are likely relevant for extrapolation of initial-state showering effects to the LHC, given the large phase space available for jet production, and relatively small ratio of jet transverse energy to the center-of-mass energy.

Refs. [1, 34] investigate the effects of corrections to collinear-ordered showers on angular and momentum correlations. Fig. 5 shows results from the collinear Herwig Monte Carlo [35] and from the $k_\perp$-shower Cascade Monte Carlo [36] for the distribution in $\Delta\phi$ and the distribution in Δp_t, measuring the transverse momentum imbalance between the leading jets. The largest differences between the two Monte Carlos are at small $\Delta\phi$ and small Δp_t, where the two highest E_T jets are away from the back to back region and one has effectively three hard, well-separated jets. By examining the angular distribution of the third jet, Ref. [1] finds significant contributions from regions where the transverse momenta in the initial state shower are not ordered. The description of the measurement by the $k_\perp$-shower is good, whereas the collinear-based Herwig shower is not sufficient to describe the observed shape.

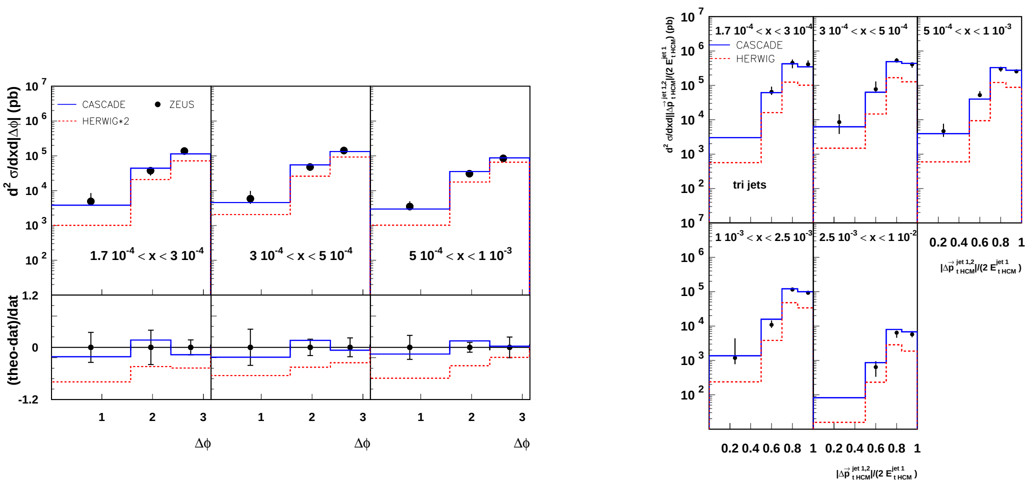

Figure 5: *(left) Angular correlations and (right) momentum correlations [1] in three-jet final states measured by [31], compared with $k_\perp$-shower (*Cascade*) and collinear-shower (*Herwig*) Monte Carlo results.*

Fig. 6 illustrates the relative contribution of matrix element corrections and shower evolution to the result [1]. The solid red curve is the full result, normalized to the back-to-back cross section. The dashed blue curve is obtained from the same unintegrated pdf's but by taking the collinear approximation in the hard matrix element. The dashed curve drops much faster than the full result as $\Delta\phi$ decreases, indicating that the high-$k_\perp$component in the hard ME is necessary to describe jet correlations for small $\Delta\phi$. The dotted (violet) curve is the result obtained from the unintegrated pdf without any resolved branching. This represents the contribution of the intrinsic $k_\perp$distribution only, corresponding to nonperturbative, predominantly low-$k_\perp$modes. That is, in the dotted (violet) curve one retains an intrinsic $k_\perp \neq 0$ but no effects of coherence. We see that the resulting jet correlations in this case are down by an order of magnitude. The inclusion of the perturbatively computed high-$k_\perp$ correction distinguishes the calculation [1] of multi-jet cross sections from shower approaches that include transverse momentum dependence in the pdfs but not in the matrix elements.

The above observations underline the role of accurate multi-jet measurements in events associated with proton scattering off virtual photons [20]. Phenomenological analyses of the available jet correlation data (and multiplicity distributions [1]) can be useful also in attempts to relate showering effects in DIS, measuring the transverse momentum in the current region [37], to vector-boson [38, 39] and scalar-boson [40] hadroproduction p_T spectra.

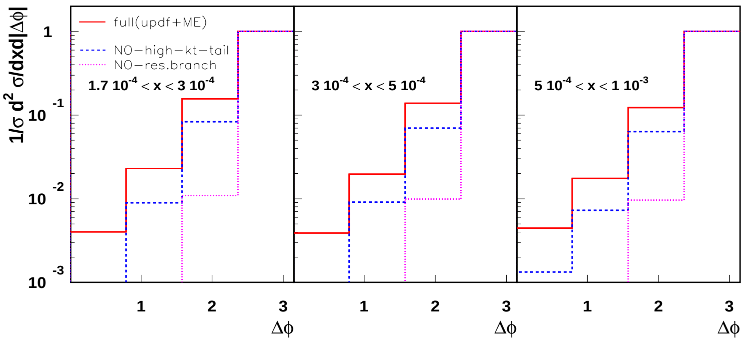

Figure 6: *The dijet azimuthal distribution [1] normalized to the back-to-back cross section: (solid red) full result (u-pdf $\oplus$ ME); (dashed blue) no finite-$k_\perp$ correction in ME (u-pdf $\oplus$ ME$_{collin.}$); (dotted violet) u-pdf with no resolved branching.*

3.2 Forward jets at the LHC

Experiments at the LHC will explore the forward region in pp collisions with the main general-purpose detectors and with dedicated instrumentation, including both proton taggers and forward calorimeters [20, 41, 42]. The forward-physics program involves a wide range of topics, from QCD to new particle discovery processes. Owing to the large center-of-mass energy of the collision and the unprecedented experimental coverage of large rapidities, it becomes possible, for the first time at hadron-hadron colliders, to carry out a program of high-p_T physics in the forward region.

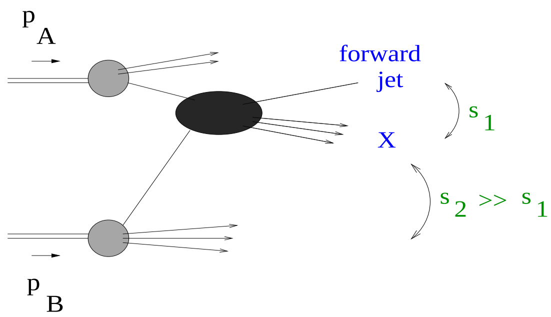

Figure 7: *Forward jet production in hadron-hadron collisions.*

The hadro-production of a forward jet associated to a hard final state X is pictured in Fig. 7. The kinematics of the process is characterized by the large ratio of sub-energies $s_2/s_1 \gg 1$ and highly asymmetric longitudinal momenta in the partonic initial state ($x_A \to 1$, $x_B \to 0$) [43].

In this kinematical region, QCD logarithmic corrections in the large rapidity interval and the hard transverse momentum may both be sizeable [2, 44]. The theoretical framework to sum consistently both kinds of logarithmic corrections to all perturbative orders is based on QCD high-energy factorization at fixed transverse momentum [19]. This factorization program is carried through in [2]. The high-energy factorized form of the forward jet cross section, differential in the final-state transverse energy Q_t and azimuthal angle φ, can be represented schematically as

$$\frac{d\sigma}{dQ_t^2 d\varphi} = \sum_a \int \ \phi_{a/A} \ \otimes \ \frac{d\widehat{\sigma}}{dQ_t^2 d\varphi} \ \otimes \ \phi_{g^*/B} \ \ , \tag{6}$$

where $\otimes$ specifies a convolution in both longitudinal and transverse momenta, $\widehat{\sigma}$ is the hard scattering cross section, calculable from a suitable off-shell continuation of perturbative matrix elements [2], $\phi_{a/A}$ is the distribution of parton a obtained by near-collinear shower evolution, and $\phi_{g^*/B}$ is the gluon unintegrated distribution obtained from $k_\perp$-dependent parton branching.

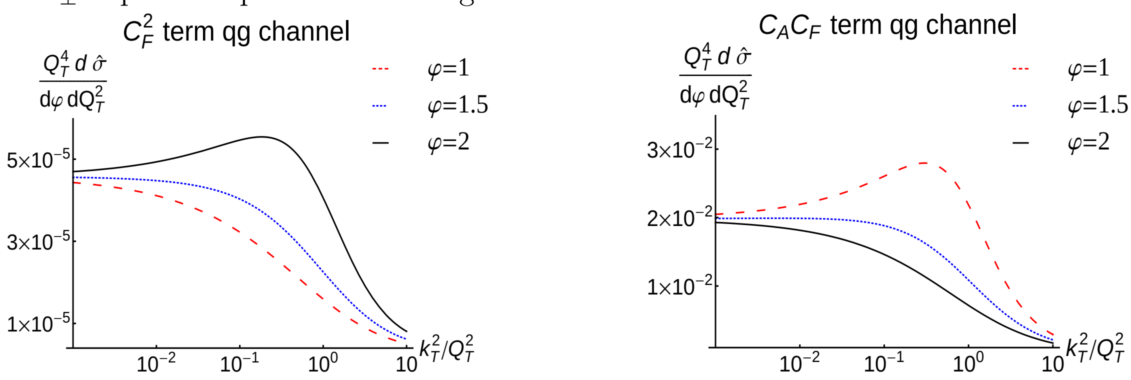

Figure 8: *Transverse momentum dependence of the factorizing short distance matrix elements [44].*

The multi-parton matrix elements [2] factorize, in the high-energy limit, not only in the collinear emission region but also at finite angle. They can be used to take into account effects of coherence from multi-gluon emission away from small angles, which become important for correlations among jets across long separations in rapidity.

Potentially significant coherence effects involve both the short-distance factor $\widehat{\sigma}$ and the long-distance factor ϕ. Fig. 8 [44] illustrates the effect in the short distance part. Here we consider the term $a = q$ in Eq. (6), and plot the cross section versus the ratio between k_t, measuring the transverse momentum carried away by additional jets accompanying the two leading jets, and Q_t, defined in terms of the transverse momenta of the hardest jets.

We observe in Fig. 8 that the role of coherence from multi- gluon emission is to set the dynamical cut-off at values of k_t of order Q_t. Non-negligible effects arise at high energy from the finite-k_t tail. These effects are not included in collinear-branching generators, and become more and more important as the jets are observed at large rapidity separations. Monte Carlo implementations of Eq. (6) and the coherent matrix elements will be relevant for phenomenological studies of the forward region.

4 Summary

Final states with high jet multiplicities acquire qualitatively new features at the LHC compared to previous collider experiments, as the phase space opens up for events characterized by multiple hard scales, possibly widely disparate from each other. This brings in potentially new effects in both the hard-scattering and the parton-shower components of the process.

If large-angle multigluon radiation gives significant contributions to parton showers, appropriate generalizations of parton branching methods are required. We have discussed applications of transverse-momentum dependent kernels for parton showering, which follow from high-energy factorization properties of QCD multiparton matrix elements.

Using precise *ep* data on three-jet final states, we observe significant corrections associated with coherent gluon radiation in the $x \ll 1$ space-like shower, arising from regions in which the partonic lines along the decay chain in the initial state are not ordered in transverse momentum. This gives rise to quite distinctive features in the jet angular correlations.

We have described a theoretical framework to incorporate coherence effects that will influence the distributions of jets produced in the forward region at the LHC. Monte Carlo implementations of this approach will be relevant for phenomenological studies of forward physics.

The coherence effects from highly off-shell processes discussed in this article can also affect the detailed structure of final-state distributions associated with heavy particle production. Monte Carlo event generators taking this into account will thus be helpful if one is to use jets as a tool to analyze potential effects of new physics at the LHC from highly boosted massive states.

References

[1] F. Hautmann and H. Jung, JHEP **0810** (2008) 113.

[2] M. Deak, F. Hautmann, H. Jung and K. Kutak, JHEP **0909** (2009) 121.

[3] B.R. Webber, CERN Academic Training Lectures (2008).

[4] R.K. Ellis, W.J. Stirling and B.R. Webber, *QCD and collider physics*, CUP 1996.

[5] J.C. Collins, D.E. Soper and G. Sterman, Adv. Ser. Direct. High Energy Phys. 5 (1988) 1.

[6] M.H. Seymour, lectures at CTEQ School (2006).

[7] S. Frixione, CERN Academic Training Lectures (2006).

[8] A. Bassetto, M. Ciafaloni and G. Marchesini, Phys. Rept. **100** (1983) 201.

[9] Yu.L. Dokshitzer, V.A. Khoze, A.H. Mueller and S.I. Troian, *Perturbative QCD*, Ed. Frontieres, Gif-sur-Yvette (1991).

[10] V.N Gribov, Sov. J. Nucl. Phys. **5** (1967) 399; F.E. Low, Phys. Rev. **110** (1958) 974.

[11] J. Frenkel and J.C. Taylor, Nucl. Phys. **B246** (1984) 231; R. Doria, J. Frenkel and J.C. Taylor, Nucl. Phys. **B168** (1980) 93.

[12] B.R. Webber, Ann. Rev. Nucl. Part. Sci. **36** (1986) 253.

[13] Yu.L. Dokshitzer, V.A. Khoze, A.H. Mueller and S.I. Troian, Rev. Mod. Phys. **60** (1988) 373.

[14] M. Ciafaloni, in *Perturbative Quantum Chromodynamics*, ed. A.H. Mueller (World Scientific, Singapore, 1989)

[15] M. Ciafaloni, Nucl. Phys. **B296** (1988) 49.

[16] S. Catani, M. Ciafaloni and F. Hautmann, Phys. Lett. B**242** (1990) 97.

[17] G. Marchesini and B.R. Webber, Nucl. Phys. **B386** (1992) 215.

[18] F. Hautmann, Acta Phys. Polon. B **40** (2009) 2139; F. Hautmann and H. Jung, arXiv:0712.0568 [hep-ph]; arXiv:0808.0873 [hep-ph].

[19] S. Catani *et al.*, Nucl. Phys. B**366** (1991) 135; Phys. Lett. **B307** (1993) 147.

[20] Z. Ajaltouni *et al.*, arXiv:0903.3861 [hep-ph].

[21] S. Jadach and M. Skrzypek, arXiv:0909.5588 [hep-ph].

[22] A.D. Martin, M.G. Ryskin and G. Watt, arXiv:0909.5529 [hep-ph].

[23] J.C. Collins, Phys. Rev. D **65** (2002) 094016; J.C. Collins and F. Hautmann, JHEP **0103** (2001) 016; Phys. Lett. B **472** (2000) 129.

[24] S. Catani and F. Hautmann, Nucl. Phys. B**427** (1994) 475; Phys. Lett. B**315** (1993) 157.

[25] F. Hautmann, Phys. Lett. B **655** (2007) 26; arXiv:0708.1319 [hep-ph].

[26] M. Ciafaloni, Phys. Lett. B**429** (1998) 363.

[27] T. Jaroszewicz, Phys. Lett. B**116** (1982) 291.

[28] V.S. Fadin and L.N. Lipatov, Phys. Lett. B**429** (1998) 127; G. Camici and M. Ciafaloni, Phys. Lett. B**430** (1998) 349.

[29] G. Altarelli, R. Ball and S. Forte, arXiv:0901.1294 [hep-ph]; Nucl. Phys. B**799** (2008) 199; M. Ciafaloni, D. Colferai, G.P. Salam and A. Stasto, JHEP **0708** (2007) 046; R.S. Thorne, Phys. Rev. D **60** (1999) 054031; R.K. Ellis, F. Hautmann and B.R. Webber, Phys. Lett. **B** 348 (1995) 582; J. Kwiecinski, Z. Phys. **C**29 (1985) 561.

[30] V.M. Abazov *et al.* [D0 Collaboration], Phys. Rev. Lett. **94** (2005) 221801 [arXiv:hep-ex/0409040].

[31] S. Chekanov *et al.* [ZEUS Collaboration], Nucl. Phys. B **786** (2007) 152 [arXiv:0705.1931 [hep-ex]].

[32] A. Aktas *et al.* [H1 Collaboration], Eur. Phys. J. C **33** (2004) 477 [arXiv:hep-ex/0310019].

[33] M.G. Albrow *et al.* [TeV4LHC QCD Working Group], [arXiv:hep-ph/0610012].

[34] F. Hautmann and H. Jung, arXiv:0804.1746 [hep-ph].

[35] G. Corcella *et al.*, JHEP **0101** (2001) 010 [arXiv:hep-ph/0011363].

[36] H. Jung *et al.*, preprint DESY-10-107; H. Jung, Comput. Phys. Commun. **143** (2002) 100.

[37] A. Banfi, arXiv:0906.4958 [hep-ph].

[38] P.Z. Skands, arXiv:0905.3418 [hep-ph].

[39] S. Berge, P.M. Nadolski, F.I. Olness and C.P. Yuan, hep-ph/0508215.

[40] M. Deak, A. Grebenyuk, F. Hautmann, H. Jung and K. Kutak, in Proc. EDS09 Workshop (CERN, 2009); F. Hautmann, arXiv:0909.1240 [hep-ph]; Phys. Lett. B **535** (2002) 159.

[41] M. Grothe, arXiv:0901.0998 [hep-ex].

[42] D. d'Enterria, Eur. Phys. J. A **31** (2007) 816; arXiv:0911.1273 [hep-ex].

[43] A.H. Mueller and H. Navelet, Nucl. Phys. B**282** (1987) 727.

[44] M. Deak, F. Hautmann, H. Jung and K. Kutak, arXiv:0908.1870 [hep-ph]; preprint OUTP-10-07-P.